Cavity-Creating Mutations in *Pseudomonas aeruginosa* Azurin: Effects on Protein Dynamics and Stability

Edi Gabellieri,* Ettore Balestreri,* Alvaro Galli,† and Patrizia Cioni*
*Istituto di Biofisica, Consiglio Nazionale delle Ricerche, 56124 Pisa, Italy; and †Istituto di Fisiologia Clinica, Consiglio Nazionale delle Ricerche, 56124 Pisa, Italy

ABSTRACT Changes in flexibility and structural stability of *Pseudomonas aeruginosa* azurin in response to cavity-creating mutations were probed by the phosphorescence emission of Trp-48, which was deeply buried in the compact hydrophobic core of the macromolecule, and by measurements of guanidinum hydrochloride unfolding, respectively. Replacement of the bulky side chains Phe-110, Phe-29, and Tyr-108 with the smaller Ala introduced cavities at different distances from the hydrophobic core. The phosphorescence lifetime (τ_0) of Trp-48, buried inside the protein core, and the acrylamide quenching rate constant (k_q) were used to monitor local and global flexibility changes induced by the introduction of the cavity. The results of this work demonstrate the following: 1), the effect on core flexibility of the insertion of cavities is not correlated readily to the distance of the cavity from the core; 2), the protein global flexibility results are related to the cavity distance from the packed core of the macromolecule; and 3), the increase in protein flexibility does not correspond necessarily to a comparable destabilizing effect of some mutations.

INTRODUCTION

Globular proteins show a unique, well defined, packed structure. According to the x-ray structure, the protein interior seems tightly packed; calculations of the average volume packing density inside proteins show it to be close to that of organic crystals (1–3). This solid-like nature of the protein interior also has been demonstrated by compressibility measurements (4,5) and high-pressure experiments (6–8). Nevertheless, globular proteins are not static structures, and several studies have demonstrated that local and global dynamical events contribute to protein properties and functioning (9). Proteins undergo conformational changes when interacting with substrates or ligands, and they experience fluctuations of different amplitude that allow diffusion of small molecules throughout the protein matrix (10,11).

The dynamical properties of proteins are correlated directly to packing heterogeneity (12). Analysis of the atomic distributions in crystal structure shows that most proteins contain small cavities that range in size from a few to several dozen cubic angstroms. These cavities often are localized at the interfaces between secondary structure elements where the hydrogen-bonding network is completely developed and the interactions among side chains are hindered (13). The role of internal cavities in protein stability and function has been highlighted in several experimental studies (14–16). Cavity size distribution appears related to protein properties such as stiffness and stability (17). Amino acid replacement often introduces a new cavity inside the protein, thus changing the protein properties. Cavity-creating mutations in the hydrophobic core of proteins cause a loss of free energy and are usually destabilizing. The direct connection between loss in stability and size of the created cavity has been demonstrated by extensive studies of T4 lysozyme (15,18). To our knowledge, little information exists about the relevance of the cavity location for protein flexibility and stability. Understanding how the distribution of cavities affects protein properties can enable the design of proteins with specific functions and stability (19).

This study specifically examines how the distance from the protein core of relatively large cavities, created by the replacement of bulky side chains with smaller ones, affects the local and global dynamics of proteins in the long (microsecond-millisecond) timescale. In addition, we investigated the consequences of the increased flexibility due to cavity creation on the stability of the mutated protein. We chose *Pseudomonas aeruginosa* azurin as model protein for the large amount of structural and thermodynamic information available on its native and mutated forms. Azurin is a small (14,400 D) monomeric protein with an eight-stranded β-sandwich structure that is closely packed to form a highly hydrophobic core, which belongs to the class of blue copper proteins. The single Trp residue (Trp-48) deeply embedded in the hydrophobic core has rather unique fluorescence properties and serves as a natural probe of the local protein structure (20). Several mutants with native-like structures have been created and investigated in terms of stability and spectroscopic properties (21–25). Recently, a study conducted by Trp phosphorescence spectroscopy on two single-point mutants, F110S and I7S, demonstrated that cavity formation in the core of the protein caused a drastic increase of large-amplitude structural fluctuations of the whole macromolecule (26). To our knowledge, little is known until now about the effects of a cavity placed outside the tightly packed hydro-

Submitted December 18, 2007, and accepted for publication March 10, 2008.

Address reprint requests to Dr. Patrizia Cioni, Istituto di Biofisica, CNR Via G. Moruzzi, 1, 56124 Pisa, Italy. Tel.: 39-050-315-3051; Fax: 39-050-315-2760; E-mail: patrizia.cioni@pi.ibf.cnr.it.

Editor: Bertrand Garcia-Moreno.

0006-3495/08/07/771/11 $2.00

doi: 10.1529/biophysj.107.128009

phobic core on the local motions inside the protein and on the global flexibility of the macromolecule.

In this study, we constructed specific mutants of azurin to identify the possible correlations between alterations of internal flexibility/thermodynamic stability and the distance of the cavity from the hydrophobic core of the protein. We used three bulky residues—Phe-110, Phe-29, and Tyr-108—located at increasing distances from Trp-48, which lies in the protein core. Azurin dynamics were analyzed using the following measurements: 1), the room temperature Trp phosphorescence decay, which provided information on the local flexibility of the protein matrix around the chromophore (27,28); and 2), the acrylamide bimolecular phosphorescence quenching rate constant (k_q), which was correlated to the structural flexibility of the whole macromolecule (29). Mutant protein stability was studied by following the fluorescence changes upon guanidinium hydrochloride denaturation. Although there was no experimental indication that the mobility of the protein core is related to the position of the mutation, the results suggest an inverse relation between the diffusion rate of the acrylamide through the protein matrix and the distance of the cavity from the highly packed protein core. No correlation between the rigidity of the azurin structure and stability was found.

MATERIALS AND METHODS

Chemicals and reagents

All chemicals were of the highest purity grade available from commercial sources and used without further purification. Tris buffer (hydroxymethyl) aminomethane), EDTA (ethylenediaminotetracetic acid disodium salt), spectroscopic grade glycerol, $ZnCl_2$ (Suprapure) and NaCl (Suprapure) were purchased from Merck (Darmstadt, Germany). Acrylamide (>99%) was purchased from Bio-Rad Laboratories (Richmond, CA) and Gdn/HCl (guanidinium hydrochloride) was obtained from Sigma-Aldrich (Deisenhofen, Germany). The concentration of Gdn/HCl was determined by the refractive index (30) and confirmed by density measurements.

Protein expression and purification

Plasmid carrying the wild-type (WT) sequence of *P. aeruginosa* azurin was a generous gift from Professor A. Desideri (Università Tor Vergata, Rome, Italy). The F29A, F110A, and Y108A mutants were constructed using the QuickChange kit (Stratagene, LaJolla, CA). Proteins were expressed in *E. coli* strain BL21 and successively isolated and purified as described by van de Kamp et al. (31). Apo-proteins were prepared from holo azurin by potassium cyanide in 0.15 M Tris-HCl/1 mM EDTA, pH 8, followed by column chromatography (31). Zn-azurins, WT and mutants, were rebuilt from apo-azurins by the addition of $ZnCl_2$/protein in the molar ratio 2:1. Complex formation was verified by looking at the Trp fluorescence intensity in experiments of competition between Cu^{2+} and Zn^{2+}, as Cu-azurin fluorescence is strongly quenched (32).

Chemical denaturation experiments

Chemical denaturation of apo-azurins were carried out in 2 mM Tris/1 mM EDTA, pH 7.5, at 20°C, in samples containing a Gdn/HCl-NaCl salt mixture, at constant ionic strength and increasing Gdn/HCl content. Samples were incubated for 2 h before measurements. For each mutant, the denaturation process was reversible as renaturation could be achieved upon diluting the samples in buffer. Equilibrium unfolding was analyzed according to the simple two-state (N↔U) model. The fraction of native protein (f_N) was determined at each Gdn/HCl concentration from the displacement of the center of mass of the Trp fluorescence spectrum (33), as described in the next section.

Fluorescence and phosphorescence measurements

Steady-state fluorescence measurements were performed on a spectrofluorometer (LS50B; Perkin-Elmer, Norwalk, CT) at 20°C. All measurements were conducted in 2 mM Tris-HCl/1 mM EDTA, pH 7.5, at a protein concentration of 2.5 μM. Excitation was at 292 nm with an excitation and emission slit width of 5 nm. All spectra were corrected for background fluorescence and the instrument response. Quantum yields were calculated by integration of the corrected emission spectra taking into account the differences in absorbance of the samples. The center of spectral mass (ν) was defined as follows:

$$\nu = (\Sigma \nu_i F_i)/(\Sigma F_i), \quad (1)$$

where F_i is the fluorescence intensity at the wavenumber ν_i and is related to f_N as follows:

$$f_N = 1 - [1 + Q(\nu_{GdnHCl} - \nu_U)/(\nu_N - \nu_{GdnHCl})]^{-1}, \quad (2)$$

where Q is the ratio of the quantum yields of unfolded and folded protein, $(\nu)_{GdnHCl}$ is the center of spectral mass at each Gdn/HCl concentration, whereas ν_U and ν_N are the corresponding values for the unfolded and folded protein, respectively.

Free energy change ($\Delta G°$) and the m value were derived from the nonlinear least-squares fitting of f_N data:

$$f_N = 1/\{1 + \exp[-(\Delta G° - m[GdnHCl])/RT\}. \quad (3)$$

For phosphorescence measurements in fluid solution, oxygen was extensively removed by the alternative application of moderate vacuum and inlet of ultra pure N_2 (27). The sample was placed in specially designed T-shaped quartz cuvettes (5 × 5 mm optical section; Spectrosil; Hellma, Mullheim/Baden, Germany) connected to the nitrogen vacuum line (34). Samples were gently shaken for ~10 min to achieve complete exchange between O_2 and N_2. Based on the phosphorescence lifetime of the protein alcohol dehydrogenase from horse liver, which exhibits high sensitivity to O_2 quenching, this procedure lowered the O_2 level to below 2 nM. All measurements were conducted in 2 mM Tris-HCl, pH 7.5, at a protein concentration ranging from 2.5 to 5 μM. Phosphorescence measurements at low temperature (77 K) were conducted in 60/40 (v/v) glycerol/buffer (2 mM Tris-HCl, pH 7.5), at a protein concentration of 10 μM. In addition, 1 mM EDTA was always added to apo-azurin samples.

Phosphorescence spectra and decays were measured with pulsed excitation (λ_{ex} = 290 nm) on a homemade apparatus (34) that had been improved with a charge-coupled device camera (Princeton Instruments Spec-10:400B(XTE); Roper Scientific, Trenton, NJ) to enhance sensitivity to low light levels and for simultaneous acquisition of the entire spectrum. Pulsed excitation was provided by a frequency-doubled Nd:YAG pumped dye laser (Quanta Systems, Milano, Italy) with pulse duration of 5 ns, pulse frequency up to 10 Hz, and energy per pulse varying from 0.1 to 1 mJ. For spectra measurements, the emission was collected at 90° from the excitation and dispersed by a 0.3-m focal length triplet grating imaging spectrograph (SpectraPro-2300i; Acton Research, Acton, MA) with a bandpass ranging from 1.0 to 0.2 nm. The emission intensity in the range from 400 to 535 nm was monitored by a back-illuminated charge-coupled device camera (1340 × 400 pixel array; Princeton Instruments Spec-10:400B(XTE); Roper Scientific, Trenton, NJ) cooled to −60°C. In low temperature glasses, the relative intense background signal, which was due to the solvent impurities, was cut

out by opening the mechanical shutter controlling the emission to the spectrograph after a delay of 3 s from the excitation pulse. In fluid solution, where the Trp phosphorescence lifetime is shorter than the 6 s of glassy media, spectra were recorded by integrating multiple excitation pulses at a repetition frequency up to 10 Hz. To block overlapping prompt fluorescence and short-lived background luminescence from reaching the detector, the laser excitation was synchronized to a fast mechanical chopper opening the emission slit 50 μs after the laser pulse. In this work, three to four pulses were sufficient to obtain satisfactory signal/noise ratios.

Phosphorescence decays were monitored by collecting the emission at 90° from vertical excitation through a filter combination (WG405; Lot-Oriel, Milano Italy) and an interference filter (DT-Blau; Balzer, Milano, Italy) with a transmission window of 405–445 nm. The photomultiplier (EMI 9235QA; THORN EMI electron tubes, Middlesex, UK) was protected against fatigue from the intense fluorescence pulse by a gating circuit that inverted the polarity of dynodes 1 and 3 up to 1.5 ms after the laser pulse. The photocurrent signal was amplified and digitized, and multiple sweeps were averaged by a multifunction board (PCI-20428W; Intelligent Instrumentation, Tucson, AZ) using Visual Designer software (PCI-209001S version 3.0; Intelligent Instrumentation).

RESULTS

Selection of azurin mutants

Three bulky side chains, residues Tyr-108, Phe-29 and Phe-110, were substituted with the smaller Ala. The distance from Trp-48 is 8.7, 5.1, and 3.1 Å, respectively, which represents the shortest edge-to-edge separation between the atoms of the aromatic rings. Phe-110, situated in strand 7, is a highly conserved residue important for native-state stability (35). F29 lies in the β-strand 3 in the protein matrix. Tyr-108, like Phe-110, is well conserved, and the x-ray structure shows that this tyrosine, at the beginning of strand 7, is hydrogen-bonded to the backbone of a residue that is five positions upstream (Fig. 1) (36). This type of turn, called the ''tyrosine corner'', can be found in most proteins with a Greek key β-barrel fold (37).

As native copper, in reduced and oxidized states, extensively quenches the fluorescence and the phosphorescence of azurin, this study examines apo- (metal-free) and holo-azurins in which native Cu^{2+} has been substituted with nonquenching Zn^{2+}, a metal that has been shown to form an equally stable complex with the protein (38).

Protein secondary structure

The native states of the F29A and Y108A mutants were indistinguishable from that of the WT protein, as probed by near- and far-ultraviolet (UV) circular dichroism (CD) spectroscopy (E. Gabellieri, E. Balestreri, A. Galli, and P. Cioni, unpublished data). For the F110A mutant (in the apo form and in the Zn form), the far-UV CD spectrum did not show any evident change compared to WT, indicating that the secondary structure was retained. The near-UV (250–300 nm) CD spectrum, however, showed distinct differences. The bands typical of Trp (282, 290, and 292) were modified, indicating an increased mobility of the indole side chain or an increased polarity of its environment.

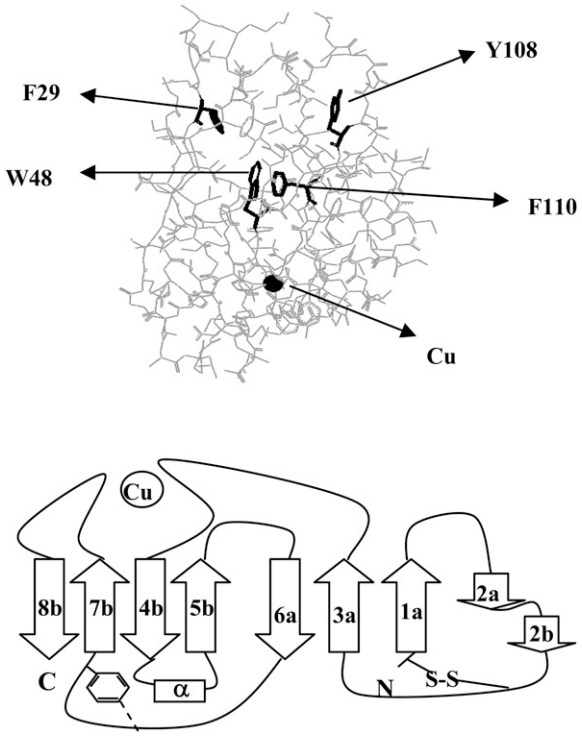

FIGURE 1 (*Left*) View of the α-carbon backbone of WT azurin from *P. aeruginosa*. The side chains of Trp-48 (W48), Phe-110 (F110), Phe-29 (F29) and Tyr-108 (Y108) are indicated in bold. (*Right*) The azurin structure represented as a topology diagram with the β-strands depicted by arrows, and the helix by a box. The two sheets are indicated with *a* and *b*. The numbering of the strands is the same as in the text.

Steady-state fluorescence spectroscopy

To our knowledge, the fluorescence spectrum peak of WT azurin (308 nm) is the most blueshifted signal observed in proteins to date. The position of the peak ($\lambda_{max} = 308$ nm) and the presence of a fine structure in the spectrum band are due to the high hydrophobicity and rigidity of the Trp-48 environment (39). Fluorescence data of the F110A, F29A, and Y108A mutants excited at 292 nm are summarized in Table 1. In comparison with native azurin, fluorescence properties were perturbed only in the F110A mutant (as previously demonstrated for the azurin mutant F110S (26)). Also in the F110A mutant, the λ_{max} was redshifted to 317 nm; the emission band was broader than the native protein ($\Delta\lambda =$ 50 nm vs. 31.5 nm of the native protein); and the quantum yield increased slightly. The addition of Zn^{2+} to rebuild the holo-proteins did not alter significantly the fluorescence emission of the different mutants (Table 1).

High-resolution phosphorescence spectra in glass matrices at 77 K

High-resolution phosphorescence spectra measured in glass matrices provided information on the polarity of surrounding groups and on the conformational homogeneity of the Trp

TABLE 1 Fluorescence characterization of WT and mutant azurins in the apo- and Zn-forms at 20°C in 20 mM KP, pH 7.5 (λ_{ex} was 292 nm)

	λ_{max} (nm)		BW* (nm)		$Q_{rel}^{\dagger}$	
Protein	apo	Zn^{2+}	apo	Zn^{2+}	Apo	Zn^{2+}
WT	308	307.5	31.5	31	1	1.06
F110A	316.5	317	50	49.5	1.24	1.14
F29A	308	307	32	31.5	1.06	1
Y108A	307.5	308	32	31.5	1.09	1.03

*BW is the width of the spectrum at half-height.

$^{\dagger}Q_{rel}$ is the quantum yield relative to native apo-azurin. Quantum yields were calculated by integration of the spectrum of protein samples with the same absorbance at 292 nm.

site. The peak wavelength of the 0,0 vibronic band ($\lambda_{0,0}$) and its bandwidth (BW, the width at half height) usually are considered to be indicators of spectral energy and broadness. The former parameter is related to the polarity of the medium around the indole ring and the latter to the homogeneity of its microenvironment. Phosphorescence spectrum of WT apo-azurin in 60/40, v/v glycerol/buffer (2 mM Tris/1 mM EDTA, pH 7.5) at 77 K exhibited a well-resolved vibrational structure (Fig. 2). Regarding the apo-WT, $\lambda_{0,0}$ was 410.4 ± 0.1 nm, a value consistent with a slightly nonpolar site (411 nm) (40). The BW was relatively large (4.17 nm) compared to sites of a structurally homogeneous protein (i.e., BW ≤ 2.11 nm of *Rhodospirillum rubrum* transhydrogenase (41)) and confirmed conformational heterogeneity in the Trp microenvironment. In each case, the replacement of Phe-110, Phe-29, and Tyr-108 with Ala caused a redshift of the spectrum (0.2 nm for F110A, a value in the order of the spectral resolution, and >2 nm for F29A and Y108A) and a further increase in BW (Fig. 3 and Table 2). The small changes in spectral energy were indicative of no evident alterations in the Trp environment, whereas the enhanced BW demonstrated greater conformational freedom in the azurin mutants. The bulky side chains of Phe-110, Phe-29, and Tyr-108 were at different distances from the indole ring. For all of them, however, the increased BW induced by their substitutions with smaller Ala verified a decrease of conformational homogeneity around the Trp.

The Zn^{2+} binding to the apo-proteins mutants enhanced the spectral resolution (Table 2), a change consistent with decreased conformational heterogeneity. These effects of the metal binding were small, practically negligible in the WT, indicating that the environment of Trp-48 in the native protein is quite similar in apo and holo structures.

Room temperature phosphorescence emission of azurins in solution

In passing from a glass state (at 77 K) to a fluid solution (at 293 K), the phosphorescence spectrum of WT azurin and mutants became broader, and the 0-0 vibrational band shifted

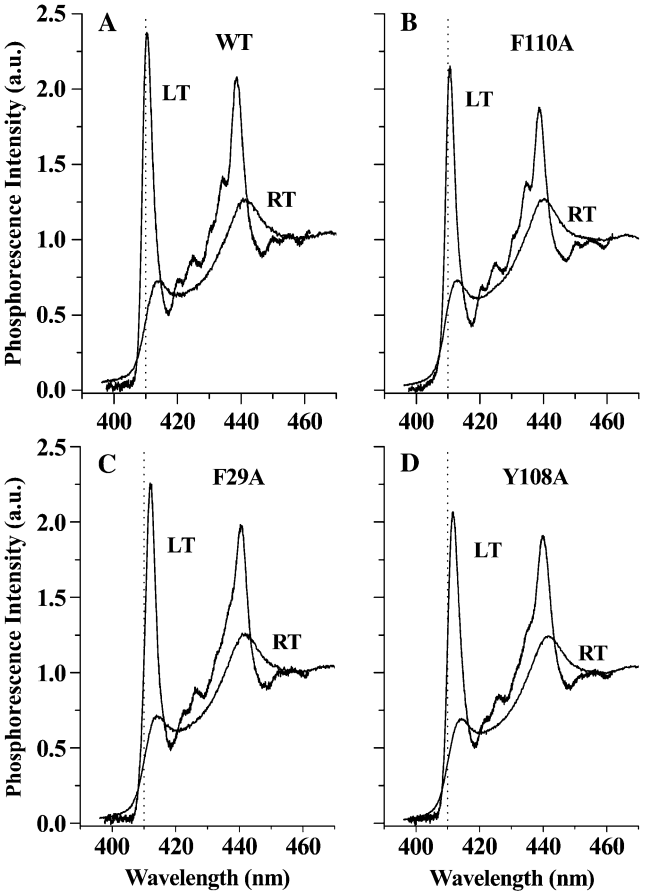

FIGURE 2 High-resolution phosphorescence spectra of apo-WT and mutant azurins in glycerol/buffer 60/40 (v/v) at 77 K (LT) and in buffer at 293 K (RT). The buffer is 2 mM Tris/1 mM EDTA, pH 7.5. Protein concentration is 10 μM. λ_{ex} is 290 nm. (*A*) WT, (*B*) F110A, (*C*) F29A, and (*D*) Y108A. In the 77 K spectra, the residual tyrosinate emission was subtracted.

to red by ~3.5 nm (Fig. 3 and Table 2), which is a typical response of thermal spectral relaxation. No significant differences of $\lambda_{0,0}$ were observed in a comparison of the room-temperature spectra of apo and holo proteins; in F110A, however, the redshift of the holo-form was smaller than that of the other proteins. In ZnF110A, a spectral redshift of only 2 nm relative to the glass state demonstrated a well-structured environment around Trp-48.

Phosphorescence decays of WT and mutant azurins (apo- and Zn-forms) in fluid solution at 20°C are shown for comparison in Fig. 3. Like the WT emission, the phosphorescence decay of the mutants were uniform and well-represented by a single lifetime. This finding is indicative of protein conformational homogeneity in the long timescale of the phosphorescence decay. In the apo-forms, mutation primarily affected the triplet decay of apoF29A, which demonstrated a considerable decrease (2.7-fold, Table 3). Binding of Zn^{2+} induced in all cases, except WT, a lengthening of the triplet state decay. The structure-tightening role of the metal ion was particularly evident in Zn-F110A, in which the phosphores-

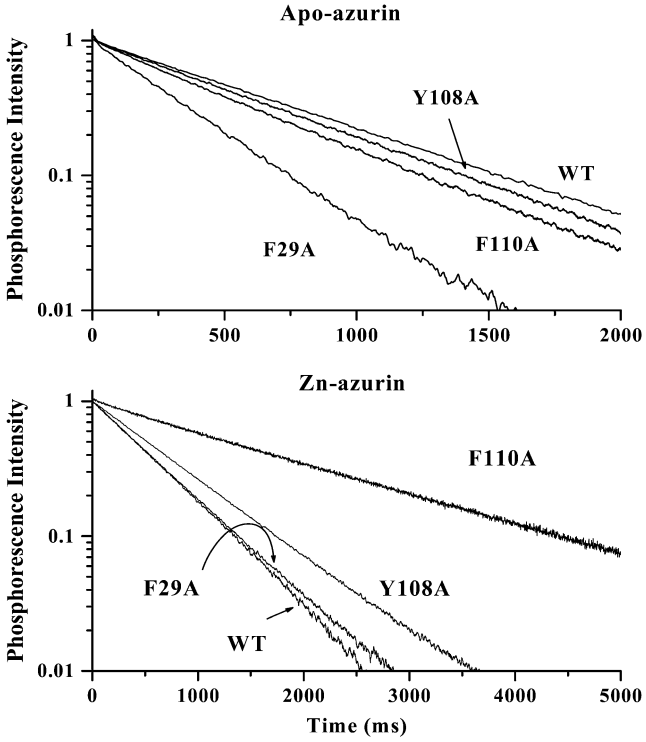

FIGURE 3 Comparison of phosphorescence decays of WT, F110A, F29A, and Y108A azurins in both apo- (*top panel*) and Zn- (*bottom panel*) forms, at 20°C. Protein concentration is typically 3–5 μM. Buffer is 2 mM Tris, pH 7.5, plus 1 mM EDTA for apo-form or 1 mM $ZnCl_2$ for Zn-form. λ_{ex} is 290 nm.

cence lifetime was 2.14 s—an increase of 4.2× compared with its apo-form and 3.5× compared with Zn-WT. Estimates of the local fluidity (η) of the Trp environment based on the relationship between the τ_0 and the solvent viscosity, derived with model compounds (27), are shown in Table 3. Because the creation of a cavity, either empty or filled with water, was expected to enhance local structural fluctuations, the long lifetime obtained with the F110A mutant, which was similar to that measured for F110S (26), is difficult to explain. It would appear that a rearrangement of the bonding network, induced by the replacement of Phe-110, further immobilizes the indole ring.

TABLE 2 Peak wavelength ($\lambda_{0\text{-}0}$) and bandwidth (BW) of the 0-0 vibronic band of the phosphorescence spectrum of WT and mutant azurins in the apo- and Zn-forms in glasses ($T = 77$ K) and in aqueous solution ($T = 20$°C)

	$T = 77$ K				$T = 20$°C	
	$\lambda_{0\text{-}0}$ (nm)		BW (nm)		$\lambda_{0,0}$ (nm)	
Protein	apo	Zn^{2+}	apo	Zn^{2+}	apo	Zn^{2+}
WT	410.4	410.5	4.17	4.17	414	414
F110A	410.6	410.6	4.30	3.88	414.5	412.8
F29A	412.3	412.0	4.75	4.12	414.6	414.3
Y108A	411.8	411.5	5.14	4.89	413.3	414.5

TABLE 3 Lifetimes obtained from the phosphorescence decay in buffer at 20°C of apo- and Zn-azurins

		τ_0 (s)		η (cP$_*10^4$)		$\Delta H^{\#}$ $(1/\eta)$ (kcal mol^{-1})	
Protein	r (Å)	Apo	Zn^{2+}	apo	Zn^{2+}	apo	Zn^{2+}
WT		0.63	0.55	5	3.8	24	24
F110A	3.1	0.53	2.20	3.45	88	32	28
F29A	5.1	0.37	0.59	1.67	4.37	25	25
Y108A	8.7	0.6	0.75	4.49	7.11	25	27

r is the shortest edge to edge separation between the atoms of the aromatic rings; η is the effective local viscosity about Trp-48 and it has been calculated according to Gonnelli and Strambini (27); $\Delta H^{\#}$ $(1/\eta)$ is the activation enthalpies obtained from the temperature dependence of $(1/\eta)$.

To estimate the activation barrier of the structural fluctuations underlying the triplet state relaxation, the lifetime in buffer was monitored across the 0–50°C temperature range. Lifetimes were converted into effective local ''viscosities'' (27) so that the parameter $(1/\eta_{prot})$ could act as an indirect measure of the rate of the structural fluctuations around Trp-48. Arrhenius plots of $\ln(1/\eta_{prot})$ vs. $1/T$ were substantially linear (Fig. 4). The activation enthalpies, $\Delta H^{\#}(1/\eta_{prot})$, derived from the slope are shown in Table 3. Activations enthalpies were large, >20 kcal/mol, suggesting that the barrier to local motions around Trp-48 involves costly rearrange-

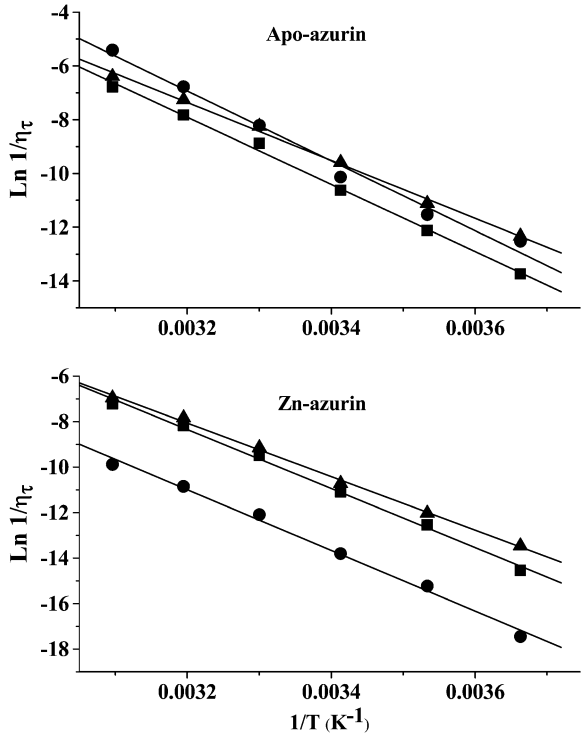

FIGURE 4 Arrhenius plots of $1/\eta_\tau$ obtained over the 0–50°C temperature range. The protein samples are (*solid squares*) Y108A, (*solid triangles*) F29A, and (*solid circles*) F110A in the apo-form (*top panel*) and Zn-form (*bottom panel*). Experimental conditions are the same as those in Fig. 3.

ments of the surrounding β-sheet in each case. It is interesting to note that, relative to the WT, differences in the activation barrier increased significantly only for the F110A mutant, both in apo- (8 kcal/mole) and holo- (4 kcal/mole) forms.

Quenching of phosphorescence by acrylamide

An independent assessment of the flexibility of the macromolecule can be obtained from the ease with which neutral quenching molecules like acrylamide have been shown to diffuse through the globular fold to the site of the chromophore and quench its phosphorescence by a relatively short-range interaction (29). Quenching experiments involve the measurement of the phosphorescence lifetime at increasing acrylamide concentrations. The bimolecular rate constant (k_q) of the reaction is obtained from the gradient of the lifetime Stern-Volmer plot ($1/\tau = 1/\tau_0 + k_q$ [acryl]). In all cases, a linear dependence of $1/\tau$ on [acryl] was found. Representative lifetime Stern-Volmer plots for quenching at 20°C are shown in Fig. 5; the magnitude of k_q calculated from the slope is shown in Table 4.

The accessibility of a large solute-like acrylamide to the tightly packed core of azurin is expected to be greatly hindered. In fact, k_q was reduced by >7/9 (apo/holo) orders of magnitude in the native protein compared to a solvent-exposed Trp residue (1.5×10^9 $M^{-1}s^{-1}$) (42). The picture

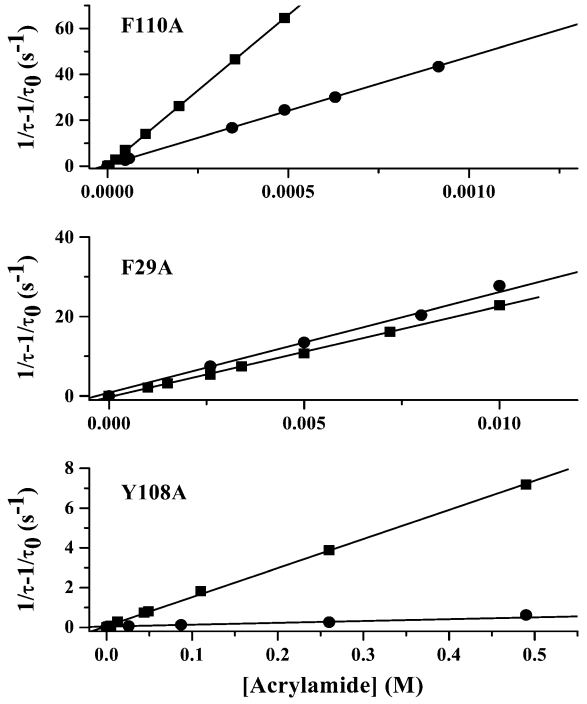

FIGURE 5 Comparison among lifetime Stern-Volmer plots for the acrylamide quenching of the azurin phosphorescence. F110A (*top*); F29A (*middle*); Y108A (*bottom*). The proteins samples are (*solid squares*) apo- and (*solid circles*) Zn-form. Experimental conditions are the same as those in Fig. 3.

changed significantly with the mutants as the substitutions of either Phe (110 and 29) with less bulky Ala, causing a dramatic enhancement up to three orders of magnitude for both mutants. In contrast, replacement of the Tyr-108 with smaller Ala did not alter significantly the permeability of the protein matrix to the acrylamide (Table 4). Interestingly, the increase in acrylamide permeability can be correlated to the proximity of the mutation site to Trp-48 (3.1, 5.1, and 8.7 Å, for Phe-110, Phe-29, and Tyr-108, respectively), thus emphasizing that the disruption of the close packing of the core region surrounding the indole ring enhances acrylamide migration to the Trp site (26). Acrylamide quenching constants confirm the important role of the metal ion in tightening the azurin structure. Relative to apo-proteins, acrylamide diffusion in Zn-proteins was slowed 3–10-fold in the F110A and Y108A mutants compared to 40-fold in the WT. The binding of Zn^{2+} to the apoF29A mutant, however, did not affect the magnitude of k_q.

As with τ_0, k_q was determined over the 0–50°C temperature range; the activation enthalpy obtained from essentially linear Arrhenius plots are shown in Table 4. The results demonstrate that, in the case of F110A, the large increase in acrylamide diffusion caused by the mutation is accompanied by a sizable, two- to three-fold reduction of the activation barrier $\Delta H^{\#}$ (k_q). In addition, Y108A shows a decrease of $\Delta H^{\#}$ (k_q) compared to the native protein (5–6 kcal mol^{-1}), suggesting that the mutation in an external site affects the structural fluctuations related to the acrylamide migration inside the protein. However, the energy barrier is similar between the apo- and holo-proteins, indicating that Zn^{2+} coordination to this mutant reduces ~2-fold k_q, primarily by an unfavorable entropic contribution. The activation barrier of k_q is surprisingly small (~1 kcal mol^{-1}) for F29A in the apo- and holo-forms (Table 4). This finding suggests that temperature-activated protein fluctuations are not involved in the quenching process; to be exact, the migration of the acrylamide inside the protein is no longer the rate-limiting step of the quenching reaction. The quenching process may be dissected into three main steps, each one of which could be rate-limiting: 1), diffusion of the acrylamide through the solvent to the protein surface; 2), migration of the quencher molecule inside the protein; and 3), the electron exchange reaction between reactants in close contact. When the quenching rate is limited by acrylamide diffusion through the solvent, the activation energy of the process is ~3.7 kcal/mol (43,44), a value more than three times greater than that measured with F29A. Specific tests performed in 40% glycerol/buffer (w/w) solution, whose viscosity at 20°C is 3.7-fold that of the buffer (45), demonstrated that the acrylamide quenching rate is practically not affected ($k_q = 2.7 \times 10^3$ $M^{-1}s^{-1}$ in 40% glycerol compared to $k_q = 2.6 \times 10^3$ in buffer). Hence, we conclude that the acrylamide diffusion through the solution is not rate-limiting. Consequently, we suggest that the rate-limiting step of the quenching reaction in F29A is the electron exchange process. Phe-29 is located

TABLE 4 Acrylamide bimolecular phosphorescence quenching constants (k_q) at 20°C and thermodynamic parameters of apo- and Zn-azurins

	k_q ($M^{-1}s^{-1}$)		$\Delta H^{\#}$ (k_q) (kcal mol^{-1})		ΔG_D (kcal mol^{-1})	m kcal $mol^{-1}M^{-1}$
Protein	apo	Zn^{2+}	apo	Zn^{2+}	apo	apo
WT	$3.2 \pm 0.5\times10^{1}$	0.8 ± 0.3	22	22	9.5 ± 0.7	4.9 ± 0.4
F110A	$1.3 \pm 0.4\times10^{5}$	$4.6 \pm 0.6\times10^{4}$	10.7	8.9	2.6 ± 0.3	3.1 ± 0.2
F29A	$2.3 \pm 0.5\times10^{3}$	$2.6 \pm 0.5\times10^{3}$	1.3	0.5	4.8 ± 0.4	4.6 ± 0.3
Y108A	$3.3 \pm 0.7\times10^{1}$	1.5 ± 0.2	17.2	16.4	1.3 ± 0.2	2.1 ± 0.1

$\Delta H^{\#}(k_q)$ is the activation enthalpy measured from the temperature dependence of k_q; ΔG_D, denaturation free energy, and m have been derived by fitting the fluorescence data as described in Materials and Methods.

5.1 Å from Trp-48, and its ring is partially exposed to the solvent. Its substitution with Ala presumably opens a cleft inside the protein matrix. Recently, it has been shown that through-space interactions between the triplet state and acrylamide occur (29), although the small magnitude of the contact rate and the attenuation length suggests that they are short-ranged. The measured value of k_q for F29A is compatible with a net separation between acrylamide and chromophore of 2.5 Å (29). Due to the cleft, presumably formed by the removal of Phe-29, the smaller space separating the aqueous phase and Trp-48 is 2–3 Å. The acrylamide in this pocket can quench effectively the triplet emission through space without further migration in the protein. In conclusion, it appears that acrylamide-quenching of F29A azurin is limited by the through-space quenching rate. In addition, the measured activation energy is the temperature dependence of the electron exchange process itself, a parameter that, to our knowledge, has not been determined before.

Influence of mutations on the stability of azurin

To test the relationship between protein stability and the above-described changes in the protein flexibility, Gdn/HCl denaturation curves were collected for the F110A, F29A, and Y108A mutants in the apo-form. The stability of the native state at 20°C was assessed from its denaturation in Gdn/HCl, as described in Materials and Methods. Equilibrium unfolding curves for WT and mutant azurins are shown in Fig. 6, and the parameters obtained by least-squares fitting of a two-state model to the data are shown in Table 4. All mutants unfold in single, reversible transitions, and the ΔG^0 is lower for all of them compared to the stability of WT azurin. The most dramatic reduction is found for the apoY108A azurin variant, which shows a $\Delta G°$ at 20°C of only 1.4 kcal/mol (9% of the protein is already denaturated at 0 M Gdn/HCl). In comparison with WT azurin, the m-value decreases significantly only for F110A and Y108A, suggesting that the change in solvent-accessible surface area of the protein during unfolding (ΔASA) is much smaller in these proteins (46,47). The dramatic decrease in the m-value for Y108A (from 4.9 in WT to 2.1 kcal mol^{-1} M^{-1}) indicates that the native form of Y108A has a greater exposed surface compared to the WT form. If this were the case, the structural changes in the mutant would be large and so evident in the spectroscopic properties. An alternative explanation for the decrease of the m-value is a deviation from a two-state unfolding mechanism that would lower the value of m (46). The substitution of a Tyr involved in a tyrosine corner has led to the occurrence of intermediate states not detected in the WT for apo-pseudoazurin (48) and neocarzinostatin (49).

DISCUSSION

From F110A to F29A and to Y108A, the created cavity is shifted, respectively, from the inner shell, to just outside the core, and to near the surface of the protein. The x-ray structures of the mutants under investigation are not available; in theory, the substitution of Phe or Tyr with Ala would create an empty space of 102 $Å^3$ and 106 $Å^3$, respectively. Although the mutant structure tends to readjust and reduce the size of

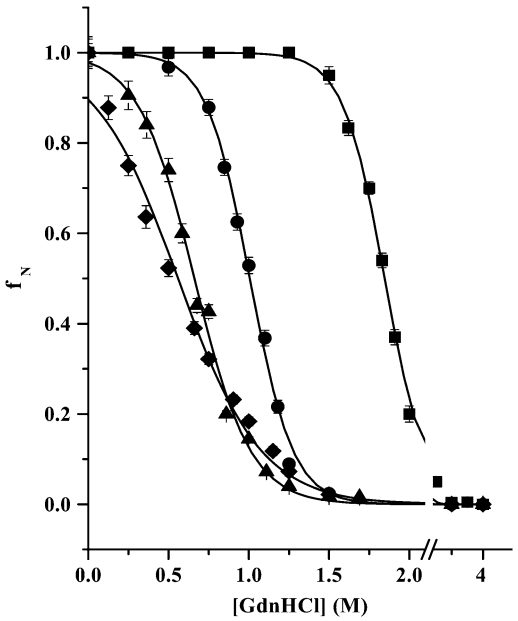

FIGURE 6 Equilibrium denaturation curves of apo-azurins in 2 mM Tris/1 mM EDTA, pH 7.5, at 20°C. The protein samples are (*solid squares*) WT, (*solid circles*) F29A, (*solid triangles*) F110A, and (*solid diamonds*) Y108A. Protein concentration was 2.5 μM anywhere. The line through the points represents the fit of the data.

the cavity to attenuate its destabilizing effects, the azurin β-scaffold is very rigid. Consequently, one would expect that the relaxation of the structure would be relatively small. The x-ray structures of two other cavity-forming azurin mutants, F110S and I7S, show cavities, apparently filled with water, of 100 $Å^3$ and 40 $Å^3$, respectively (50), volumes close to the theoretical expectations.

Effects of cavities on the local flexibility of the inner core

In azurin, the phosphorescence probe is located roughly at the center of the β-barrel, and the indole ring is surrounded by nonpolar side chains that form a compact hydrophobic core. By all criteria, including crystallographic *B*-factors (51), T1 NMR relaxation times (52), and molecular dynamics simulations (53,54), the aromatic ring is immobilized in an unusually rigid domain. Due to a rigid environment, Trp-48 exhibits a long phosphorescence lifetime (0.63 s) at ambient temperature that, translated into a local ''viscosity'', gives $\eta = 5 \times 10^4$ cP (27).

It is expected that a local probe would be influenced primarily by mutations near the probe environment, unless the replacement of the amino acid caused a consistent structural rearrangement of the macromolecule. Our results, however, show that the dependence of the distance on the local flexibility upon the introduction of a cavity is more complicated and unpredictable.

The substitution of Phe-110 with Ala creates a large cavity in the core of protein that would presuppose a consistent increase in the local fluidity. In fact, the reduction of the τ_0 of apo-F110A with respect to WT provides evidence of a more fluid Trp environment, even if the increase in fluidity is moderate. For Y108A, the triplet lifetime is practically identical to that of WT, indicating that a void inserted close to the protein surface would not affect the fluidity of the distant, embedded core. In F29A, where the cavity is located halfway between the solvent and the compact globular folds, the shortening of τ_0 confirms a much more fluid tryptophan environment relative to WT, equaling roughly a three-fold decrease in the local viscosity for the apo-protein. The gain in local flexibility measured for the F29A mutant, which is greater than that found for the F110A azurin, suggests that the insertion of a cavity in a looser packing site induces more extensive structural rearrangement than a cavity created in the highly packed core of a protein, such as F110A.

The introduction of the metal reestablishes bonds and therefore would tighten the protein structure. Metal binding, however, decreases the local flexibility in the mutated proteins, whereas it does not affect WT azurin. The lifetime of Zn-F110A (2.14 s), if translated in terms of effective viscosity, demonstrates an increase of more than 20 times in local stiffness. A glassy-like state for the Trp environment, also confirmed by the small spectral shift measured at 20°C, calls for an extensive and rigid H-bonding network involving local side chains and water molecules in the cavity. An increase of the local rigidity around Trp also has been measured in Cd-F110S, where the local viscosity increases more than 605 times compared to Cd-WT azurin. Indeed, the lifetime of Cd-F110S (3.36 s) approaches the limiting value of 6 s observed for the chromophore in rigid glass, and it is the largest yet reported, to our knowledge, for a protein in buffer at ambient temperature. It has been hypothesized that Ser110 forms a hydrogen bond with the nitrogen-containing aromatic ring of Trp-48, which is responsible for the unusual rigidity of the chromophore (26). The long lifetime, also measured for Zn-F110A, demonstrates that the matrix of the core of the protein is effectively much more rigid in the mutants where Phe is substituted. In F110S, the role of H-bond of Ser in the stiffening of the core structure, if there is one, is additional. It was pointed out to us (G. B. Strambini, Istituto di Biofisica, Consiglio Nazionale delle Ricerche, personal communication, 2006) that the crystal structure of Cu-WT azurin shows a distortion of the indole ring, presumably due to the high packing density of the site, which probably reduces the triplet lifetime of the Trp. Structure rearrangement induced by the amino acid replacement could eliminate the ring distortion and restore the unperturbed long lifetime of the holo-protein.

Effects of cavities on large-amplitude structural fluctuations

Acrylamide migration to the site of Trp-48 in WT azurin is highly hindered; an extremely small value of k_q, with a large activation barrier, is likely to reflect the scarce probability for acrylamide to reach this compact inner shell, as it requires concerted motions of large domains. The large activation barrier for k_q ($\Delta H^{\#} = 22$ kcal/mol), which is very close to the value for the relaxation of the triplet state ($\Delta H^{\#} = 24$ kcal/mol), suggests that the rate-limiting step in the migration of acrylamide to Trp-48 involves fluctuations in the inner core structure. Therefore, although the replacement of a bulky side chain with a smaller one in the inner core of the protein would favor the migration of the quencher to the spectroscopic probe, it is reasonable to expect that the insertion of cavities out of this barrier would slightly affect the permeation of the acrylamide.

Our results show that the accessibility of a large solute such as acrylamide to the compact core of azurin is sharply modulated by the presence of an internal cavity. The effect, which we interpret in terms of a change in the internal flexibility of azurin (26), is very dependent on the position of the mutation relative to the central, hydrophobic core of the protein.

Among the three mutations studied, the cavity created by replacement of Phe-110 in the azurin inner core is the most effective in increasing the rate of acrylamide migration through the globular fold, indicating a huge influence on the average dynamics of azurin. A similar result (26) also was obtained for other two core variants of azurin, F110S and I7S.

This suggests that cavities engineered in compact globular folds considerably enhance large-amplitude structural fluctuations and, consequently, the permeability of the macromolecule to large solutes. The relationship between cavity and increased mobility already has been proposed in previous studies on L99A, a Leu-Ala cavity mutant of T4 lysozyme (55–58). The ^{15}N-relaxation dispersion NMR spectroscopy demonstrated that microsecond-millisecond timescale motion in regions proximal to Leu-Ala substitution, presumably related to the rapid exchange in and out of molecules such as benzene or xenon and not detected in the WT protein, are due to the cavity (56). In the L99A T4 lysozyme, the increased mobility of several side chains coexist with an unexpected structural rigidity of the peptide backbone around the cavity, which retains its overall size under pressures above 100 MPa (6). Similarly, Zn-F110A and Cd-F110S azurin mutants present a more rigid protein core, as revealed by the slower triplet state decay rate, but an enhancement of the protein matrix large-amplitude fluctuations as indicated by the increase of the acrylamide permeability.

Results obtained with Y108A, in which the cavity created was exposed to the solvent, indicate that even superficial, local conformational changes may have effects at long distances on the migration of solutes (substrates, effectors) to internal active sites.

Because the quenching rate is determined by a through-space interaction, for F29A, it is not possible to derive direct information on the effects of the mutation on protein dynamics; only an upper limit can be given to the acrylamide migration rate of 2.3×10^3 $M^{-1}s^{-1}$. This magnitude is considerably lower than the value of k_q ($1.3 \times 10^5 M^{-1}s^{-1}$) for F110A. It also proves that the position of the engineered cavity, right into the protein for F110A as opposed to a shallower site for F29A, is critical for the impact it may have on protein flexibility.

Effects of cavity position on azurin stability

Globular proteins are characterized by the specific and tight binding of hydrophobic side chains in the so-called hydrophobic core that play a key role in the stability of proteins (59). Mutations that introduce smaller side chains in hydrophobic cores generally tend to destabilize proteins (15,59,60), and it is expected that the thermodynamic consequences of the creation of cavities depend on the proximity of the mutation to the protein core. According to these expectations, the decrease in stability of F110A and F29A appears to be greater as the site of perturbation is closer to the hydrophobic core, whereas the dramatic loss of ΔG measured for Y108A ($\Delta\Delta G \sim 8$ kcal/mol) is unexpected. Tyr-108 is an exposed residue, and its removal does not change the overall structural and dynamical features of the protein. We attribute the remarkable decrease in stability to the removal of the hydrogen bond of the tyrosine corner due to the mutation. The removal of this connection has been shown to be important for the stability and, in some cases, for the folding of Greek key β-barrel proteins (48,61).

Although one expects that the insertion of cavities would be less penalized in protein stability when moving toward the protein surface, our results indicate that this can only be a weak correlation. Depending on the nature of the bonds that are broken by the amino acid substitution, the change in stability can be very large even for superficial sites.

Various studies suggest a correlation between protein stability and protein flexibility (62–65). Recent work, however, indicates that this interrelationship may not be straightforward (66–68). Phosphorescence parameters, τ_0 and k_q, demonstrate large-amplitude structural fluctuations (in a timescale from milliseconds to seconds) believed to be essential for protein function (69–71). Our data do not show a correlation between azurin structure rigidity and stability. In fact, the local flexibility parameter τ_0 indicates F29A as the most flexible azurin, but its stability is the highest among the mutants. In contrast, regarding both the core and the average flexibility as measured by τ_0 and k_q, Y108A is practically identical to WT. Its stability, however, is lower, and it is already partly denaturated in the absence of denaturants. Yet, it is possible that the lack of correlation found between flexibility and stability in our study could be due to the local nature of our probe.

In conclusion, our work emphasizes that engineered cavities can affect large-amplitude structural fluctuations and, consequently, the permeability of the macromolecule to large solutes, and that their influence is strongly dependent on the distance of the cavity from the site of the probe. In contrast, the effect on core flexibility of the insertion of cavities is unpredictable, depending on the distance of the cavity from the protein core and on local factors. Furthermore, the results reported in our study draw attention to the fact that the effect on protein stability depends sharply on the nature of the bonds broken by the mutation.

The authors thank Dr. Giovanni Strambini for helpful discussions and for critical reading of the manuscript, and A. Puntoni and G. Chiti for technical assistance.

REFERENCES

1. Harpaz, Y., M. Gerstein, and C. Chothia. 1994. Volume changes on protein folding. *Structure*. 2:641–649.
2. Richards, F. M. 1974. The interpretation of protein structures: total volume, group volume distributions and packing density. *J. Mol. Biol.* 82:1–14.
3. Richards, F. M. 1977. Areas, volumes, packing and protein structure. *Annu. Rev. Biophys. Bioeng.* 6:151–176.
4. Gavish, B., E. Gratton, and C. J. Hardy. 1983. Adiabatic compressibility of globular proteins. *Proc. Natl. Acad. Sci. USA.* 80:750–754.
5. Kharakoz, D. P., and A. P. Sarvazyan. 1993. Hydrational and intrinsic compressibilities of globular proteins. *Biopolymers.* 33:11–26.
6. Collins, M. D., M. L. Quillin, G. Hummer, B. W. Matthews, and S. M. Gruner. 2007. Structural rigidity of a large cavity-containing protein revealed by high-pressure crystallography. *J. Mol. Biol.* 367:752–763.
7. Kauzmann, W., K. Moore, and D. Schultz. 1974. Protein densities from x-ray crystallographic coordinates. *Nature.* 248:447–449.

8. Kundrot, C. E., and F. M. Richards. 1987. Crystal structure of hen egg-white lysozyme at a hydrostatic pressure of 1000 atmospheres. *J. Mol. Biol.* 193:157–170.
9. McCammon, J. A., and S. C. Harvey. 1987.Dynamics of Proteins and Nucleic Acids. Cambridge University Press. Cambridge, MA.
10. Collins, M. D., G. Hummer, M. L. Quillin, B. W. Matthews, and S. M. Gruner. 2005. Cooperative water filling of a nonpolar protein cavity observed by high-pressure crystallography and simulation. *Proc. Natl. Acad. Sci. USA.* 102:16668–16671.
11. Igumenova, T. I., K. K. Frederick, and A. J. Wand. 2006. Characterization of the fast dynamics of protein amino acid side chains using NMR relaxation in solution. *Chem. Rev.* 106:1672–1699.
12. Halle, B. 2002. Flexibility and packing in proteins. *Proc. Natl. Acad. Sci. USA.* 99:1274–1279.
13. Kocher, J. P., M. Prévost, S. J. Wodak, and B. Lee. 1996. Properties of the protein matrix revealed by the free energy of cavity formation. *Structure.* 4:1517–1529.
14. Desjarlais, J. R., and T. M. Handel. 1995. De novo design of the hydrophobic cores of proteins. *Protein Sci.* 4:2006–2018.
15. Eriksson, A. E., W. A. Baase, X. J. Zhang, D. W. Heinz, M. Blaber, E. P. Baldwin, and B. W. Matthews. 1992. Response of a protein structure to cavity-creating mutations and its relation to the hydrophobic effect. *Science.* 255:178–183.
16. Jackson, S. E., M. Moracci, N. elMasry, C. M. Johnson, and A. R. Fersht. 1993. Effect of cavity-creating mutations in the hydrophobic core of chymotrypsin inhibitor 2. *Biochemistry.* 32:11259–11269.
17. Graziano, G. 2007. Cavity size distribution in the interior of globular proteins. *Chem. Phys. Lett.* 434:316–319.
18. Xu, J. A., W. A. Baase, E. Baldwin, and B. W. Matthews. 1998. The response of T4 lysozyme to large-to-small substitutions within the core and its relation to the hydrophobic effect. *Protein Sci.* 7:158–177.
19. Sibille, N., A. Favier A. I. Azuaga, G. Ganshaw, R. Bott, A. M. Bonvin, R. Boelens, and N. A. van Nuland. 2006. Comparative NMR study on the impact of point mutations on protein stability of *Pseudomonas mendocina* lipase. *Protein Sci.* 15:1915–1927.
20. Finazzi-Agrò A., G. Rotilio, L. Avigliano, P. Guerrieri, V. Boffi, and B. MondovÌ. 1970. Environment of copper in *Pseudomonas fluorescens* azurin: fluorometric approach. *Biochemistry.* 9:2009–2014.
21. Guzzi, R., L. Sportelli, C. La Rosa, D. Milardi, D. Grasso, M. Ph. Verbeet, and G. W. Canters. 1999. A spectroscopic and calorimetric investigation on the thermal stability of the Cys3Ala/Cys26Ala azurin mutant. *Biophys. J.* 77:1052–1063.
22. Pozdnyakova, I., J. Guidry, and P. Wittung-Stafshede. 2001. Copper stabilizes azurin by decreasing the unfolding rate. *Arch. Biochem. Biophys.* 390:146–148.
23. Pozdnyakova, I., J. Guidry, and P. Wittung-Stafshede. 2002. Studies of *Pseudomonas aeruginosa* azurin mutants: cavities in beta-barrel do not affect refolding speed. *Biophys. J.* 82:2645–2651.
24. Pozdnyakova, I., and P. Wittung-Stafshede. 2001. Copper binding before polypeptide folding speeds up formation of active (holo) *Pseudomonas aeruginosa* azurin. *Biochemistry.* 40:13728–13733.
25. Pozdnyakova, I., and P. Wittung-Stafshede. 2001. Biological relevance of metal binding before protein folding. *J. Am. Chem. Soc.* 123:10135–10136.
26. Cioni, P., E. de Waal, G. W. Canters, and G. B. Strambini. 2004. Effects of cavity-forming mutations on the internal dynamics of azurin. *Biophys. J.* 86:1149–1159.
27. Strambini, G. B., and M. Gonnelli. 1995. Tryptophan phosphorescence in fluid solution. *J. Am. Chem. Soc.* 117:7646–7651.
28. Gonnelli, M., and G. B. Strambini. 1995. Phosphorescence lifetime of tryptophan in proteins. *Biochemistry.* 34:13847–13857.
29. Cioni, P., and G. B. Strambini. 1998. Acrylamide quenching of protein phosphorescence as a monitor of structural fluctuations in the globular fold. *J. Am. Chem. Soc.* 120:11749–11757.
30. Strambini, G. B., and M. Gonnelli. 2007. Protein stability in ice. *Biophys. J.* 92:2131–2138.
31. van de Kamp, M., M. C. Silvestrini, M. Brunori, J. Van Beeumen, F. C. Hali, and G. W. Canters. 1990. Involvement of the hydrophobic patch of azurin in the electron-transfer reactions with cytochrome *c*551 and nitrite reductase. *Eur. J. Biochem.* 194:109–118.
32. Strambini, G. B., and E. Gabellieri. 1991. Phosphorescence from Trp-48 in azurin: influence of Cu(II), Cu(I), Ag(I), and Cd(II) at the coordination site. *J. Phys. Chem.* 95:4352–4356.
33. Mei, G., A. Di Venere, F. Malvezzi Campeggi, G. Gilardi, N. Rosato, F. De Matteis, and A. Finazzi-Agrò. 1999. The effect of pressure and guanidine hydrochloride on azurins mutated in the hydrophobic core. *Eur. J. Biochem.* 265:619–626.
34. Strambini, G. B., B. A. Kerwin, B. D. Mason, M. Gonnelli. 2004. The triplet-state lifetime of indole derivatives in aqueous solution. *Photochem. Photobiol.* 80:462–470.
35. Wilson, C. J., and P. Wittung-Stafshede. 2005. Role of structural determinants in folding of the sandwich-like protein *Pseudomonas aeruginosa* azurin. *Proc. Natl. Acad. Sci. USA.* 102:3984–3987.
36. Leckner, J. 2001.Folding and structure of azurin—The influence of a metal. PhD thesis. Chalmers University of Technology, Göteborg, Sweden.
37. Hemmingsen, J. M., K. M. Gernert, J. S. Richardson, and D. C. Richardson. 1994. The tyrosine corner: a feature of most Greek key beta-barrel proteins. *Protein Sci.* 3:1927–1937.
38. Engeseth, H. R., and D. R. McMillin. 1986. Studies of thermally induced denaturation of azurin and azurin derivatives by differential scanning calorimetry: evidence for copper selectivity. *Biochemistry.* 25:2448–2455.
39. Gilardi, G., G. Mei, N. Rosato, G. W. Canters, and A. Finazzi-Agrò. 1994. Unique environment of Trp48 in *Pseudomonas aeruginosa* azurin as probed by site-directed mutagenesis and dynamic fluorescence spectroscopy. *Biochemistry.* 33:1425–1432.
40. Galley, W. C., and G. B. Strambini. 1976. Kinetics of triplet-triplet energy transfer and intramolecular distances in enzyme-inhibitor complexes. *Nature.* 261:521–522.
41. Broos, J., E. Gabellieri, G. I. van Boxel, J. B. Jackson, and G. B. Strambini. 2003. Tryptophan phosphorescence spectroscopy reveals that a domain in the NAD(H)-binding component (dI) of transhydrogenase from *Rhodospirillum rubrum* has an extremely rigid and conformationally homogeneous protein core. *J. Biol. Chem.* 278:47578–47584.
42. Kerwin, B. A. B. S. C., C. V. Gegg, M. Gonnelli, T. Li, and G. B. Strambini. 2002. Interaction between PEG and type I soluble tumor necrosis receptor: modulation by pH and by PEGylationat the N-terminus. *Protein Sci.* 11:1825–1833.
43. Punyiczki, M., and A. Rosenberg. 1992. The effect of viscosity on the accessibility of the single tryptophan in human serum albumin. *Biophys. Chem.* 42:93–100.
44. Eftink, M. R., and C. A. Ghiron. 1976. Exposure of tryptophanyl residues in proteins. Quantitative determination by fluorescence quenching studies. *Biochemistry.* 15:672–680.
45. Miner, C. S., and N. N. Dalton. 1953. Glycerol. Reinhold Publishers, New York.
46. Myers, J. K., C. N. Pace, and J. M. Scholtz. 1995. Denaturant m values and heat capacity changes: relation to changes in accessible surface areas of protein unfolding. *Protein Sci.* 4:2138–2148.
47. Courtenay, E. S., M. W. Capp, R. M. Saecker, and M. T. Record Jr. 2000.Thermodynamic analysis of interactions between denaturants and protein surface exposed on unfolding: interpretation of urea and guanidinium chloride m-values and their correlation with changes in accessible surface area (ASA) using preferential interaction coefficients and the local-bulk domain model. *Proteins.* 41 (Suppl. S4):72–85.
48. Jones, S., J. S. Reader, M. Healy, A. P. Capaldi, A. E. Capaldi, A. E. Ashcroft, A. P. Kalverda, D. A. Smith, and S. E. Radford. 2000. Partially unfolded species populated during equilibrium denaturation of the beta-sheet protein Y74W apo-pseudoazurin. *Biochemistry.* 39: 5672–5682.

49. Nicaise, M., M. Valerio-Lepiniec, N. Izadi-Pruneyre, E. Adjadj, P. Minard, and M. Desmadril. 2003. Role of the tyrosine corner motif in the stability of neocarzinostatin. *Protein Eng.* 16:733–738.
50. Hammann, C., A. Messerschmidt, R. Huber, H. Nar, G. Gilardi, and G. W. Canters. 1996. X-ray crystal structure of the two site-specific mutants Ile7Ser and Phe110Ser of azurin from *Pseudomonas aeruginosa*. *J. Mol. Biol.* 255:362–366.
51. Nar, H., A. Messerschmidt, R. Huber, M. van de Kamp, and G. W. Canters. 1991. Crystal structure analysis of oxidized *Pseudomonas aeruginosa* azurin at pH 5.5 and pH 9.0. A pH-induced conformational transition involves a peptide bond flip. *J. Mol. Biol.* 221:765–772.
52. Mei, G., M. Venanzi, N. Rosato, G. W. Canters, and A. F. Agro. 1996. Probing the structure and mobility of *Pseudomonas aeruginosa* azurin by circular dichroism and dynamic fluorescence anisotropy. *Protein Sci.* 5:2248–2254.
53. Arcangeli, C., A. R. Bizzarri, and S. Cannistraro. 1999. Long-term molecular dynamics simulation of copper azurin: structure, dynamics and functionality. *Biophys. Chem.* 78:247–257.
54. Arcangeli, C., A. R. Bizzarri, and S. Cannistraro. 2001. Concerted motions in copper plastocyanin and azurin: an essential dynamics study. *Biophys. Chem.* 90:45–56.
55. Mulder, F. A., B. Hon, D. R. Muhandiram, F. W. Dahlquist, and L. E. Kay. 2000. Flexibility and ligand exchange in a buried cavity mutant of T4 lysozyme studied by multinuclear NMR. *Biochemistry.* 39: 12614–12622.
56. Mulder, F. A., N. R. Skrynnikov, B. Hon, F. W. Dahlquist, and L. E. Kay. 2001. Measurement of slow (micros-ms) time scale dynamics in protein side chains by (15)N relaxation dispersion NMR spectroscopy: application to Asn and Gln residues in a cavity mutant of T4 lysozyme. *J. Am. Chem. Soc.* 123:967–975.
57. Mulder, F. A., B. Hon, A. Mittermaier, F. W. Dahlquist, and L. E. Kay. 2002. Slow internal dynamics in proteins: application of NMR relaxation dispersion spectroscopy to methyl groups in a cavity mutant of T4 lysozyme. *J. Am. Chem. Soc.* 124:1443–1451.
58. Quillin, M. L., W. A. Breyer, I. J. Griswold, and B. W. Matthews. 2000. Size versus polarizability in protein-ligand interactions: binding of noble gases within engineered cavities in phage T4 lysozyme. *J. Mol. Biol.* 302:955–977.
59. Vlassi, M., G. Cesareni, and M. Kokkinidis. 1999. A correlation between the loss of hydrophobic core packing interactions and protein stability. *J. Mol. Biol.* 285:817–827.
60. Buckle, A. M., P. Cramer, and A. R. Fersht. 1996. Structural and energetic responses to cavity-creating mutations in hydrophobic cores: observation of a buried water molecule and the hydrophilic nature of such hydrophobic cavities. *Biochemistry.* 35:4298–4305.
61. Hamill, S. J., E. Cota, C. Chothia, and J. Clarke. 2000. Conservation of folding and stability within a protein family: the tyrosine corner as an evolutionary cul-de-sac. *J. Mol. Biol.* 295:641–649.
62. Collins, T., M. A. Meuwis, C. Gerday, and G. Feller. 2003. Activity, stability and flexibility in glycosidases adapted to extreme thermal environments. *J. Mol. Biol.* 328:419–428.
63. Tsai, A. M., T. J. Udovic, and D. A. Neumann. 2001. The inverse relationship between protein dynamics and thermal stability. *Biophys. J.* 81:2339–2343.
64. Zavodszky, P., J. Kardos, A. Svingor, and G. A. Petsko. 1998. Adjustment of conformational flexibility is a key event in the thermal adaptation of proteins. *Proc. Natl. Acad. Sci. USA.* 95:7406–7411.
65. Tang, K. E., and K. A. Dill. 1998. Native protein fluctuations: the conformational-motion temperature and the inverse correlation of protein flexibility with protein stability. *J. Biomol. Struct. Dyn.* 16:397–411.
66. Hernandez, G., F. E. Jenney Jr., M. W. Adams, and D. M. LeMaster. 2000. Millisecond time scale conformational flexibility in a hyperthermophile protein at ambient temperature. *Proc. Natl. Acad. Sci. USA.* 97:3166–3170.
67. Fitter, J., R. Herrmann, N. A. Dencher, A. Blume, and T. Hauss. 2001. Activity and stability of a thermostable alpha-amylase compared to its mesophilic homologue: mechanisms of thermal adaptation. *Biochemistry.* 40:10723–10731.
68. Grottesi, A., M. A. Ceruso, A. Colosimo, and A. Di Nola. 2002. Molecular dynamics study of a hyperthermophilic and a mesophilic rubredoxin. *Proteins.* 46:287–294.
69. Amadei, A., A. B. Linssen, and H. J. Berendsen. 1993. Essential dynamics of proteins. *Proteins.* 17:412–425.
70. de Groot, B. L., S. Hayward, D. M. F. van Aalten, A. Amadei, and H. J. C. Berendsen. 1998. Domain motions in bacteriophage T4 lysozyme: a comparison between molecular dynamics and crystallographic data. *Proteins.* 31:116–127.
71. Bahar, I., A. R. Atilgan, M. C. Demirel, and B. Erman. 1998. Vibrational dynamics of folded proteins: significance of slow and fast motions in relation to function and stability. *Phys. Rev. Lett.* 80:2733–2736.